1. N. A. Shairi[1], 2. F. N. M. Yasin[1], 3. A. Othman[1], 4. Z. Zakaria[1], 5. I. M. Ibrahim[1], 6. H. A. Majid[2], 7. M. H. Jamaluddin[3], 8. A. M. Ibrahim[4]

Microwave Research Group, Centre for Telecommunication Research & Innovation (CeTRI),
Fakulti Kejuruteraan Elektronik dan Kejuruteraan Komputer (FKEKK), Universiti Teknikal Malaysia Melaka (UTeM), Malaysia (1)
Faculty of Engineering Technology, Universiti Tun Hussein Onn Malaysia (UTHM), Malaysia (2)
Wireless Communication Centre (WCC), Universiti Teknologi Malaysia (UTM), Malaysia (3)
Al-Nisour University College, Baghdad, Iraq (4)
ORCID: 1. 0000-0002-4611-5116; 2. 0000-0003-0585-3996; 3. 0000-0002-3814-1488; 4. 0000-0003-1467-405X, 5. 0000-0002-7177-0542
6. 0000-0003-2144-8579, 7. 0000-0002-1577-4047

Design and Analyses of Reconfigurable Dumbbell-Shaped and Modified H-Shaped DGSs in Millimeter Wave Band

Abstract. The design and analyses of reconfigurable dumbbell-shaped and modified H-shaped Defected Ground Structures (DGS) in the millimeter wave band (26/28 GHz band) are presented in this paper. The proposed DGSs were designed to be a reconfigurable between bandstop and allpass responses that would be used for 5G interference mitigation and as well as in RF switch design. In the design process, a mathematical model was developed for the analysis of reconfigurable capability between these two responses. Then, based on the E and H field concentration in the electromagnetic (EM) simulation, a suitable location of a PIN diode for the electronically controlled between bandstop and allpass was physically identify on the proposed reconfigurable DGS. Finally, a preliminary verification with an ideal PIN diode (open and short circuited) on the fabricated design was validated with the simulation results. Results showed that the proposed reconfigurable DGS can be changed between bandstop and allpass. The attenuation of the bandstop was more than -20 dB and the insertion loss of the allpass was lower than -3 dB in the 26/28 GHz band.

Streszczenie. W artykule przedstawiono projektowanie i analizy rekonfigurowalnych i zmodyfikowanych struktur naziemnych w kształcie hantli (DGS) w paśmie fal milimetrowych (pasmo 26/28 GHz). Proponowane systemy gwarancji depozytów zostały zaprojektowane tak, aby były rekonfigurowalne między pasmowym zatrzymaniem a wszystkimi odpowiedziami przejścia, które byłyby wykorzystywane do łagodzenia zakłóceń 5G, a także do projektowania przełączników RF. W procesie projektowania opracowano model matematyczny do analizy rekonfigurowalnych możliwości między tymi dwiema odpowiedziami. Następnie, w oparciu o stężenie pola E i H w symulacji elektromagnetycznej (EM), odpowiednia lokalizacja diody PIN dla elektronicznie sterowanego między pasmowym ogranicznikiem a wszystkimi przejściami została fizycznie zidentyfikowana na proponowanym rekonfigurowalnym DGS. Na koniec wstępna weryfikacja z idealną diodą PIN (otwartą i zwartą) na wytworzonej konstrukcji została zweryfikowana wynikami symulacji. Wyniki pokazały, że proponowany rekonfigurowalny system DGS można zmieniać między bandstopem a all pass. Tłumienie ogranicznika pasma było większe niż 20 dB, a tłumienie wtrąceniowe wszystkich przebiegów było mniejsze niż -3 dB w paśmie 26/28 GHz. (Projektowanie i analizy rekonfigurowalnych systemów DGS w kształcie hantli i zmodyfikowanych systemów DGS w kształcie litery H w paśmie fal milimetrowych)

Keywords: defected ground structure; millimeter wave; reconfigurable DGS.
Słowa kluczowe: uszkodzona struktura gruntu; fala milimetrowa; rekonfigurowalny system DGS.

Introduction

Defected ground structure (DGS) is popularly used in high frequency (radio frequency spectrum) such as filters [1-4], antenna [5-7], power amplifier [8-10], switches [11], and power divider [12-14]. The use of the DGS in these circuits has its different purposes such as isolation [6, 9], load matching network [8], miniaturization [2, 12, 13], harmonics or frequency suppression [2, 10, 12], and wideband performance [5, 9, 14].

On the other hand, in designing a wireless communication system, engineers have always had to worry about interference from both outside sources and other users of the wireless technology. In order to accurately recover the sent information, the classical wireless communications design cycle has included monitoring or forecasting channel impairments, selecting a modulation strategy, signal preconditioning at the transmitter, and processing at the receiver. Therefore, several interferences in wireless communication have been discussed such as WLAN [15], Bluetooth [16] and fifth generation (5G) [17].

Currently, 5G millimetre wave technologies have taken centre stage in the growth of the information and telecommunications industry. The need for increased data rates and the allocation of a spectrum band at higher frequencies (in millimeter wave) have led to the development of complicated and dynamic wireless communication systems [18]. As reported in [19], it was demonstrated that the fixed-satellite service (FSS) experiences interference from numerous IMT-2020s (5G communication standard) in the millimetre wave band. Therefore, this new implementation will conflict with the existing technologies.

To reduce any potential interference, a cognitive radio (CR) is required in 5G millimetre wave communications. As a result, there are several techniques of interference mitigation in CR systems, including multi-hop multiple input multiple output (MIMO) decode-and-forward relaying protocol [20], spectrum sharing [21, 22], interference mitigation in ultra-wideband (UWB) receiver architecture by exploiting the spatial and spectral diversity [23], user clustering and resource allocation in NOMA [24], cooperative spectrum sensing [25], interference management technique in device-to-device (D2D) applications [26, 27]. In addition, reconfigurable circuit components such as filters [17] and antennas [7, 28, 29] are required in front-end CR systems in order to support multichannel, multiband, and multifunctional operations while also offering an interference mitigation solution. To physically suppress interference in the front-end receiver, these techniques are known as an active interference cancellation [23]. Therefore, as mentioned in [17, 28], device controls utilizing PIN or varactor diodes are necessary.

In the reconfigurable or switchable filtering methods that can be applied in a CR system, the filter response can be changed from bandpass to bandstop [30-33] and from bandstop to allpass [34-36]. A variety of resonators such as T-type inductive coupling structure [32], microstrip line lossy resonators [33], evanescent-mode cavity resonator [34], substrate integrated waveguide (SIW) resonator [35] and acoustic-wave-lumped-element resonator [36] were implemented in the switchable/reconfigurable filter designs.

In this paper, two types of defected ground structure (DGS) which are dumbbell-shaped and modified H-shaped were designed to be a reconfigurable between bandstop

and allpass responses in the millimeter wave band (26/28 GHz band). The proposed DGSs would be used for 5G interference mitigation in CR systems. In the design process, a mathematical model was developed for the analysis of reconfigurable capability between these two responses. Then, an EM simulation was performed in order to physically identify a suitable location of the PIN diode for the electronically controlled between bandstop and allpass. This is based on the E and H field concentration on the proposed reconfigurable DGS. Finally, a preliminary verification with an ideal PIN diode (open and short circuited) on the fabricated design was carried out for validating between measurement and simulation results.

Besides, in the near future, the proposed designs have a potential to be used in RF switch design for wireless communications such as 4G and 5G as discussed in [11, 37]. This is the fact that, the proposed reconfigurable DGS is the same concept of using any switchable resonator in RF switch design as reported in [38-40].

Mathematical Analysis of a Reconfigurable DGS

In this section, a reconfigurable DSG model as shown in Figure 2 is discussed via a mathematical analysis. The analysis is based on two conditions: bandstop and allpass responses. The reconfigurable DSG model is an equivalent circuit of DGS (L and C) using a PIN diode (D), that can be switched between bandstop and allpass responses.
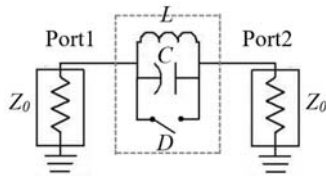
Fig. 1. Reconfigurable DGS equivalent circuit of parallel L and C with PIN diode switch.

The equivalent circuit of DGS is a simple parallel L and C. Thus, the DGS impedance is calculated as

$$(1) \quad Z_{DGS} = jX_{LC}$$

$$= \frac{\left(\frac{1}{j\omega C}\right)(j\omega L)}{\left(\frac{1}{j\omega C}\right)+(j\omega L)} = \frac{j\omega L}{1+\omega^2 LC}.$$

Now, consider the PIN diode in OFF state, which ideally be an open circuit of the DGS. As a result, the DGS will act as a bandstop response. Then, the DGS's transmission matrix ($ABCD$) is

$$(2) \quad T_{DGS} = \begin{bmatrix} 1 & Z_{DGS} \\ 0 & 1 \end{bmatrix} = \begin{bmatrix} 1 & \left(\frac{j\omega L}{1+\omega^2 LC}\right) \\ 0 & 1 \end{bmatrix}$$

The bandstop response of S_{21} is then derived from (2) using conversion between $ABCD$ and S-parameter to

$$(3) \quad S_{21} = \frac{2}{A+\frac{B}{Z_0}+Z_0 C+D} = \frac{2}{2+\frac{j\omega L}{(1-\omega^2 LC)Z_0}+Z_0}$$

where Z_0 is a characteristic impedance of the input and output of the DGS. Referring to (3), if $Z_0 = 1$ which is a normalize impedance, L and C will produce a bandstop response. Therefore, a resonant frequency is produced when

$$(4) \quad j\omega L - \frac{j}{\omega c} = 0.$$

Thus,

$$(5) \quad f_o = \frac{1}{2\pi LC}$$

where f_o is the resonant frequency in Hertz (Hz).

The following allpass response analysis is considered at the PIN diode in an ON state. In this analysis, the DGS should ideally be short circuited. As a result, the DGS responds as an allpass response. Theoretically, the allpass response can be produced if at least one or both of the components of L and C are zero. Therefore, if C is removed by short circuited of the PIN diode, C will become zero. Then let $Z_0 = 1$, which is a normalized impedance, thus S_{21} of (3) becomes

$$(6) \quad S_{21} = \frac{2}{2+\frac{j\omega L}{(1-\omega^2 L(0))}+1} = \frac{2}{3} \approx 1$$

or in decibel (dB), which is

$$(7) \quad |S_{21}|^2 dB = 20\log_{10}(1) = 0\ dB\ .$$

From (7), it is clear that an ideal zero insertion loss can be obtained, producing an allpass response.

Based on the mathematical analyses, additional analysis in electronic design automation (EDA) software (for instance, CST Microwave Studio) is required to the proposed DGS in order to make it electronically reconfigurable between bandstop and allpass responses. Indentification of the effective location of the PIN diode on the DGS is needed in the EDA software. This analysis is important so that it will tally with the mathematical analysis of the equivalent circuit of the reconfigurable DGSs.
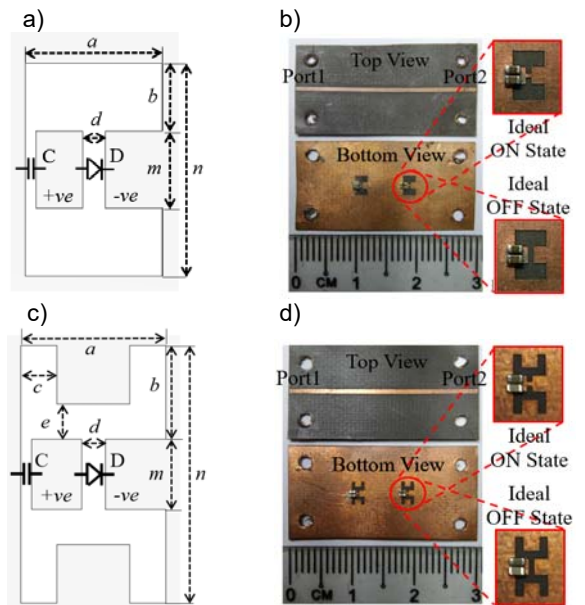
Fig. 2. Dimensions and the fabricated DGSs for (a) Design A: dimension, (b) Design A: prototype, (c) Design B: dimension, (d) Design B: prototype.

Reconfigurable DGS Design for Dumbbell-Shaped and Modified H-Shaped

To design the reconfigurable DGS circuit, the concept of an ideal switch is used. Each DGS is presented by two layouts, which are open circuited condition (active DGS) and short circuited condition (inactive DGS). The active DGS produces bandstop response due to OFF state of the PIN diode and the inactive DGS produces allpass response due to ON state of the PIN diode. Figure 2(a) shows the dimensions of the dumbbell-shaped DGS (denoted as Design A) and Figure 2(b) shows the fabricated prototype of the DGS. Figure 2(c) and Figure 2(d) show the dimensions of the modified H-shaped DGS (denoted as Design B) and the photograph of the fabricated DGS, respectively. A summary of the dimensions is shown in Table 1.

As can be seen in the Figure 2(a) and 2(c), the location of the PIN diode in the DGSs was identified based on the EM simulation for the E and H field. This simulation results are discussed in the Results and Discussion section. Besides, capacitor (C) is also used as a DC block to create a small positive (+ve) area of voltage supply to the anode of the PIN diode (D).

For validation, Design A and B were fabricated using Roger RT/Duroid 5880 with 0.254 mm thickness and relative dielectric constant of 2.2. Each prototype (the bottom view) consists of a cascaded two DGSs with 6 mm distance to provide a higher bandstop response. Therefore, the overall dimension of the fabricated design is 30 mm x 15 mm = 450 mm^2. The top view is a microstrip line with 50 Ω impedance in 26/28 GHz band. The insertion loss, attenuation and return loss performances of the fabricated DGSs were measured using the Microwave Network Analyzer which connected to a high precision cable.

Table 1. Dimension of Design A and Design B

Parameters	Dimensions [mm]	
	Design A	Design B
a	2	2
b	1	1.34
c	-	0.5
d	0.3302	0.3302
e	-	0.5
m	1.13	1
n	3.13	3.68

Results and Discussion

CST Microwave Studio was used to simulate the electromagnetic (EM) field distribution of Design A and Design B at the centre frequency of 27 GHz in the 26/28 GHz band. Figure 3(a) is the E-field concentration for Design A (left) and Design B (right). Meanwhile, Figure 3(b) is the H-field concentration for Design A (left) and Design B (right).

a)

b)
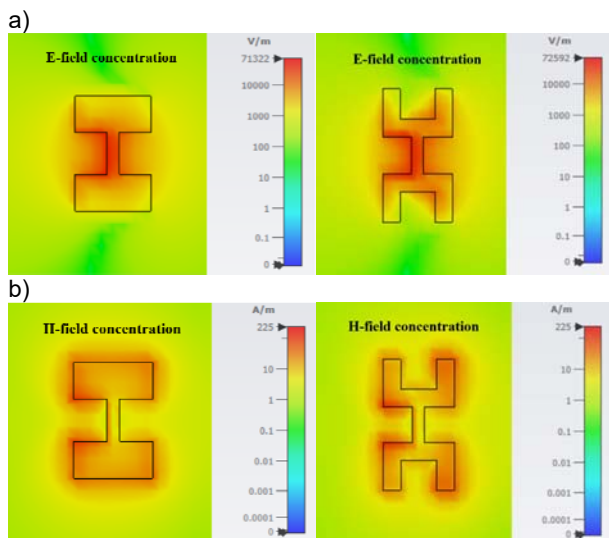
Fig. 3. Simulated EM field distribution of the reconfigurable DGSs for the concentration of (a) E-field and (b) H-field.

It was found that the concentration of E-field was mainly located in the middle of the structure of Design A and B. Meanwhile, the H-field was concentrated almost equally surrounding of the structures. Take note that the E-field is related to the capacitance and the H-field is related to the inductance of the DGSs. Thus, if referring to the mathematical analysis, the most practical to reconfigure between bandstop and allpass is by disturbing the E-field of the DGS which is related to the capacitor element. This can

be referred to (6) and (7). Therefore, a PIN diode should be put in the middle of the DGS with a suitable d, that is not longer than the length of the PIN diode package.

Figure 4 (a) and (b) show the simulated and measured results of the reconfigurable DGS for both Design A and Design B during the active DGS (which is an ideal OFF state of the PIN diode). The results produced a bandstop response with more than 20 dB of attenuation (S21) in the 26/28 GHz band. Comparing between Design A and B, it can be seen that Design A is almost comparable between simulation and measurement results. Besides, it showed that the maximum notch (simulation) was at 26.8 GHz for Design A and 29.1 GHz for Design B, respectively. Meanwhile, the return loss (S11) was very close to the 0 dB.

a)

b)
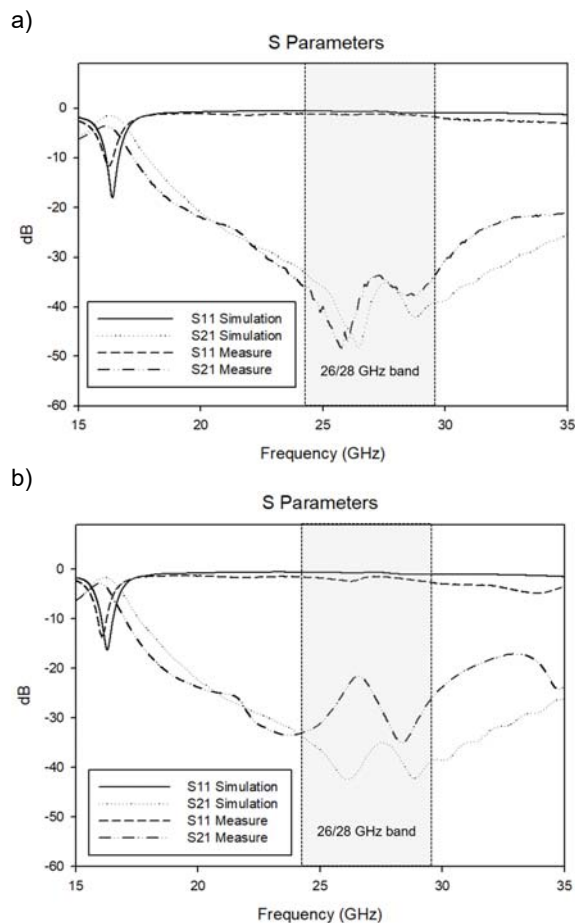
Fig. 4. Bandstop response of reconfigurable DGSs for (a) Design A (b) Design B.

a)
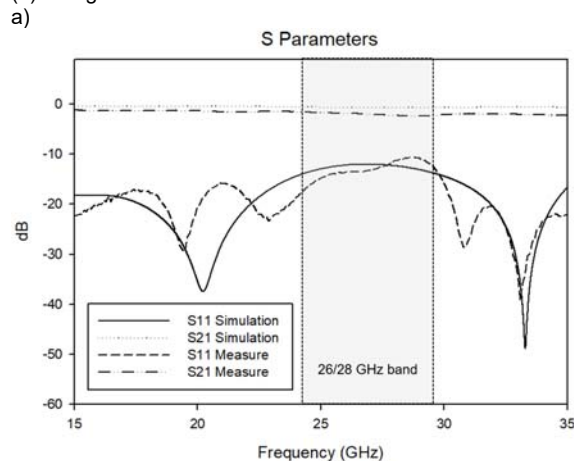
b)
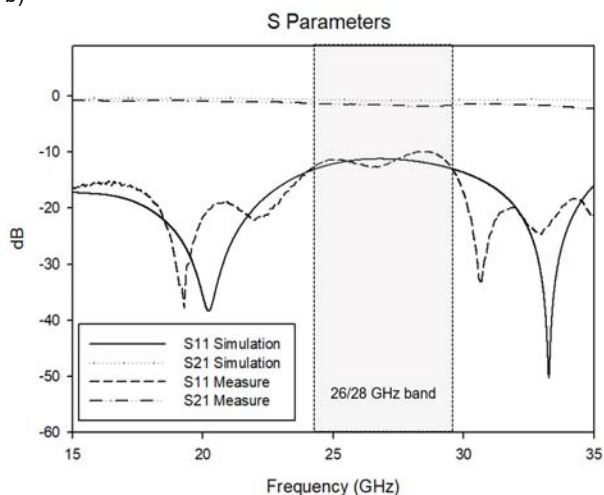
Fig. 5. Allpass response of reconfigurable DGSs for (a) Design A (b) Design B.

The simulated and measured results of the reconfigurable DGS during the inactive DGS (which is an ideal ON state of the PIN diode) are shown in Figure 5 (a) and (b). The results produced an allpass response with less than 3 dB of insertion loss (S21) in the 26/28 GHz band. Meanwhile the return loss (S11) was higher than -10 dB across the band. The measurement and simulation results are almost comparable for both Design A and B.

Table 2 below shows the summarized of the performance comparison between measurement and simulation results for the Design A and B. In general, all the measured results of design A and B were tallied and comparable with the simulated results, except for the bandstop response (attenuation) for Design B (the difference with 13.49 dB). This could be due to the fabrication or the assembly of the design. The next step for the proposed reconfigurable DGS is to implement the actual PIN diode with a biasing circuit for the ON and OFF state operations. The PIN diode is a package type that can be soldered on the printed circuit board of the DGS.

Table 2. Insertion loss, attenuation and return loss performances at 27 GHz (center of 26/28 GHz band)

DGS Design		Allpass Response (ON state)		Bandpass Response (OFF state)	
		Insertion Loss (S21 in dB)	Return Loss (S11 in dB)	Attenuation (S21 in dB)	Return Loss (S11 in dB)
Design A	Simulation	0.69	11.93	39.31	0.63
	Measured	1.98	13.30	33.92	1.19
Design B	Simulation	0.78	11.25	37.02	0.67
	Measured	1.60	12.22	23.53	1.55

Conclusion

The proposed reconfigurable DGSs using dumbbell-shaped and modified H-shaped for millimeter wave in 26/28 GHz were designed and a simple mathematical modelling was discussed for the bandstop and allpass responses. Based on the mathematical analysis, the DGS can be switched to allpass if at least one or both of the components of L and C are zero. Then, the simulated E-field and H-field were analyzed and, it was found that the PIN diode location can be determined by referring to the maximum E-field concentration compared to the H-field. Finally, the proposed reconfigurable DGSs were fabricated using the Rogers RT/Duroid 5880 material and the measured results were tallied with simulated results and were performed based on the ideal ON and OFF states of the PIN diode. These designs could be used in cognitive radio systems for the 5G interference mitigation and as well as in RF switch design.

Authors: The first five authors are from the same university and faculty, which is Universiti Teknikal Malaysia Melaka (UTeM), Jalan Hang Tuah Jaya, 76100 Durian Tunggal, Melaka, Malaysia. Their emails are as follows:
Dr. Noor Azwan Shairi, E-mail: noorazwan@utem.edu.my;
Fatin Nadiah Mohd Yasin, E-mail: m022110026@student.utem.edu.my;
Prof. Dr. Zahriladha Zakaria, E-mail: zahriladha@utem.edu.my;
Adib Othman, E-mail: adib@utem.edu.my;
Assoc. Professor Dr. Imran Mohd Ibrahim, E-mail: imranibrahim@utem.edu.my;

Dr. Huda A Majid, Faculty of Engineering Technology, Universiti Tun Hussein Onn Malaysia (UTHM), Malaysia, E-mail: mhuda@uthm.edu.my;

Assoc. Professor Dr. Mohd Haizal Jamaluddin, Wireless Communication Centre (WCC), Universiti Teknologi Malaysia (UTM), Malaysia, Email: haizal@utm.edu.my.
Dr. Ayman Mohammed Ibrahim, Al-Nisour University College, Baghdad, Iraq. Email: ayman971972@gmail.com.

REFERENCES

[1] Muchhal, Nitin, Arnab Chakraborty, Tanvi Agrawal, and Shweta Srivastava. "Miniaturized and selective half-mode substrate integrated waveguide bandpass filter using Hilbert Fractal for sub-6 GHz 5G applications." *IETE Journal of Research* (2022): 1-8.

[2] Zakaria, Z., N. A. Shairi, R. Sulaiman, and W. Y. Sam. "Design of reconfigurable defected ground structure (DGS) for UWB application." In *2012 IEEE Asia-Pacific Conference on Applied Electromagnetics (APACE)*, pp. 195-198. IEEE, 2012.

[3] Mahant, Keyur, and Hiren Mewada. "Substrate Integrated Waveguide based dual-band bandpass filter using split ring resonator and defected ground structure for SFCW Radar applications." *International Journal of RF and Microwave Computer-Aided Engineering* 28, no. 9 (2018): e21508.

[4] Yee, See Khee, Soon Chong Johnson Lim, Pih Shyan Pong, and Samsul Haimi Dahlan. "Microstrip defected ground structure for determination of blood glucose concentration." *Progress In Electromagnetics Research C* 99 (2020): 35-48.

[5] Shah, Shaharil Mohd, M. Mohamad, S. A. Hamzah, Z. Z. Abidin, F. C. Seman, N. Katiran, H. A. Majid, A. Ashyap, and S. Mohamad. "A 2.45 GHz microstrip antenna with harmonics suppression capability by using defected ground structure." *Bulletin of Electrical Engineering and Informatics* 9, no. 1 (2020): 387-395.

[6] Jabire, Adamu Halilu, Anas Abdu, Sani Saminu, Abubakar Muhammad Sadiq, and Mohammed Jajere Adamu. "Isolation Frequency Switchable MIMO Antenna for PCS, WIMAX and WLAN Application." *ELEKTRIKA-Journal of Electrical Engineering* 18, no. 3 (2019): 27-33.

[7] Riaz, Sharjeel, Xiongwen Zhao, and Suiyan Geng. "A frequency reconfigurable MIMO antenna with agile feedline for cognitive radio applications." *International Journal of RF and Microwave Computer‐Aided Engineering* 30, no. 3 (2020): e22100.

[8] Komarov, Vasyl, Oleksii Barybin, and Yulia V. Rassokhina. "Low-Pass Load Matching Network Design Using Dumbbell-Shaped DGS for High-Efficiency Microwave Power Amplifiers." In *2019 International Conference on Information and Telecommunication Technologies and Radio Electronics (UkrMiCo)*, pp. 1-4. IEEE, 2019.

[9] Alngar, Omar Z., Adel Barakat, and Ramesh K. Pokharel. "High PAE CMOS Power Amplifier With 44.4% FBW Using Superimposed Dual-Band Configuration and DGS Inductors." *IEEE Microwave and Wireless Components Letters* 32, no. 12 (2022): 1423-1426.

[10] Rassokhina, Yulia V., Dmitrii V. Chernov, and Paolo Colantonio. "High-Efficiency Microwave Power Amplifier with Higher Harmonics Level Control on Basis of Defected Ground Structure Resonators." In *2020 23rd International Microwave and Radar Conference (MIKON)*, pp. 88-91. IEEE, 2020.

[11] Othman, A., H. A. Majid, N. A. Shairi, A. A. Zolkefli, N. Al-Fadhali, Z. Z. Abidin, I. M. Ibrahim, and Z. Zakaria. "Millimeter-Wave SPDT Discrete Switch Design with Reconfigurable Circle Loaded Dumbbell DGS." In *2022 International Workshop on Antenna Technology (iWAT)*, pp. 49-52. IEEE, 2022.

[12] Khare, Ajay, Santosh Kharat, Akshay Rajapkar, S. M. Rathod, and Makarand Kulkarni. "Design of a Compact Wilkinson Power Divider using Four Asymmetric DGS for Harmonic Suppression." In *2019 TEQIP III Sponsored International Conference on Microwave Integrated Circuits, Photonics and Wireless Networks (IMICPW)*, pp. 353-356. IEEE, 2019.

[13] Farooq, Memoona, Amber Abdullah, M. Ayaz Zakir, and Hammad M. Cheema. "Miniaturization of a 3-way power divider using defected ground structures." In *2019 IEEE Asia-Pacific Microwave Conference (APMC)*, pp. 1503-1505. IEEE, 2019.

[14] Tian, Zhen, Yunbo Rao, Zhixian Deng, and Xun Luo. "Reconfigurable Dual-Band Filtering Power Divider With Ultra-Wide Stopband Using Hybrid Microstrip/Square Defected Ground Structure." In *2019 IEEE MTT-S International Microwave Symposium (IMS)*, pp. 428-431. IEEE, 2019.

[15] Zankiewicz, Andrzej. "Susceptibility of IEEE 802.11 n networks to adjacent-channel interference in the 2.4 GHz ISM band." *Przeglad Elektrotechniczny* 88, no. 9b (2012): 287-288.

[16] Pang, Bozheng, Tim Claeys, Davy Pissoort, Hans Hallez, and Jeroen Boydens. "A Study on the Impact of the Number of Devices on Communication Interference in Bluetooth Low Energy." In *2020 XXIX International Scientific Conference Electronics (ET)*, pp. 1-4. IEEE, 2020.

[17] Islam, Hashinur, Saumya Das, Tanushree Bose, and Tanweer Ali. "Diode based reconfigurable microwave filters for cognitive radio applications: A review." *IEEE Access* 8 (2020): 185429-185444.

[18] Choudhury, Debabani. "5G wireless and millimeter wave technology evolution: An overview." In *2015 IEEE MTT-S International Microwave Symposium*, pp. 1-4. IEEE, 2015.

[19] Cho, Yeongi, Hyun-Ki Kim, Maziar Nekovee, and Han-Shin Jo. "Coexistence of 5G with satellite services in the millimeter-wave band." *IEEE Access* 8 (2020): 163618-163636.

[20] Tin, Phu Tran, Duy-Hung Ha, Pham Minh Quang, Nguyen Thanh Binh, and Nguyen Luong Nhat. "Performance of multi-hop cognitive MIMO relaying networks with joint constraint of intercept probability and limited interference." *TELKOMNIKA (Telecommunication Computing Electronics and Control)* 19, no. 1 (2021): 44-50.

[21] Saleh, Mohammed Mehdi, Ahmed A. Abbas, and Ahmed Hammoodi. "5G cognitive radio system design with new algorithm asynchronous spectrum sensing." *Bulletin of Electrical Engineering and Informatics* 10, no. 4 (2021): 2046-2054.

[22] Hattab, Ghaith, Eugene Visotsky, Mark C. Cudak, and Amitava Ghosh. "Uplink interference mitigation techniques for coexistence of 5G millimeter wave users with incumbents at 70 and 80 GHz." *IEEE Transactions on Wireless Communications* 18, no. 1 (2018): 324-339.

[23] Siafarikas, Dimitrios, Elias A. Alwan, and John L. Volakis. "Interference mitigation for 5G millimeter-wave communications." *IEEE Access* 7 (2018): 7448-7455.

[24] Ali, Konpal Shaukat, Hesham Elsawy, Anas Chaaban, and Mohamed-Slim Alouini. "Non-orthogonal multiple access for large-scale 5G networks: Interference aware design." *IEEE Access 5* (2017): 21204-21216.

[25] Toma, Ogeen H., and Miguel López-Benítez. "Cooperative spectrum sensing: A new approach for minimum interference and maximum utilisation." In *2021 IEEE International Conference on Communications Workshops (ICC Workshops)*, pp. 1-6. IEEE, 2021.

[26] Sarma, Subhra S., and Ranjay Hazra. "Interference mitigation methods for D2D communication in 5G network." In *Cognitive Informatics and Soft Computing*, pp. 521-530. Springer, Singapore, 2020.

[27] Siddiqui, Maraj Uddin Ahmed, Faizan Qamar, Faisal Ahmed, Quang Ngoc Nguyen, and Rosilah Hassan. "Interference management in 5G and beyond network: Requirements, challenges and future directions." *IEEE Access* 9 (2021): 68932-68965.

[28] Bri, Seddik, and Adil Saadi. "Reconfigurable ultra wideband to narrowband antenna for cognitive radio applications using PIN diode." *TELKOMNIKA (Telecommunication Computing Electronics and Control)* 18, no. 6 (2020): 2807-2814.

[29] Ahmad, Khalid Subhi, and Mohamad Zoinol Abidin Abd Aziz. "Frequency reconfigurable microstrip antenna array based on reconfigurable defected ground structure." *Przegląd Elektrotechniczny* 97 (2021).

[30] Kingsly, Saffrine, Malathi Kanagasabai, M. Gulam Nabi Alsath, Sangeetha Subbaraj, and Sandeep Kumar Palaniswamy. "Switchable Resonator Based Reconfigurable Bandpass/Bandstop Microstrip Filter." *International Journal of Electronics* 108, no. 9 (2021): 1610-1622.

[31] Narayana, Shriman, and Yatendra Kumar Singh. "Dual-band bandpass to bandstop switchable filter with independently tunable center frequency and bandwidth." *Microwave and Optical Technology Letters* 63, no. 11 (2021): 2704-2709.

[32] Fan, Maoyu, Kaijun Song, Yu Zhu, and Yong Fan. "Compact bandpass-to-bandstop reconfigurable filter with wide tuning range." *IEEE Microwave and Wireless Components Letters* 29, no. 3 (2019): 198-200.

[33] Zahari, M. K., B. H. Ahmad, and N. A. Shairi. "Comparison of Electronically Switchable High Q Bandstop to Bandpass Filters Based on Allpass Network." In *2021 IEEE Symposium on Wireless Technology & Applications (ISWTA)*, pp. 43-47. IEEE, 2021.

[34] Guyette, Andrew C., Eric J. Naglich, and Sanghoon Shin. "Switched allpass-to-bandstop absorptive filters with constant group delay." *IEEE Transactions on Microwave Theory and Techniques* 64, no. 8 (2016): 2590-2595.

[35] Zolkefli, Amirul Aizat, Noor Azwan Shairi, Badrul Hisham Ahmad, Adib Othman, Nurulhalim Hassim, Zahriladha Zakaria, Imran Mohd Ibrahim, and Huda A. Majid. "Switchable bandstop to allpass filter using cascaded transmission line SIW resonators in K-band." *Bulletin of Electrical Engineering and Informatics* 10, no. 5 (2021): 2617-2626.

[36] Psychogiou, Dimitra. "Reconfigurable all-pass-to-bandstop acoustic-wave-lumped-element resonator filters." *IEEE Microwave and Wireless Components Letters* 30, no. 8 (2020): 745-748.

[37] Shairi, N. A., Z. Zakaria, A. M. S. Zobilah, B. H. Ahmad, and P. W. Wong. "Design of SPDT switch with transmission line stub resonator for WiMAX and LTE in 3.5 GHz band." *ARPN J. Eng. Appl. Sci* 11, no. 5 (2016): 3198-3202.

[38] Meng, Fanyi, Kaixue Ma, Kiat Seng Yeo, Chirn Chye Boon, Wei Meng Lim, and Shanshan Xu. "A 220–285 GHz SPDT switch in 65-nm CMOS using switchable resonator concept." *IEEE Transactions on Terahertz Science and Technology* 5, no. 4 (2015): 649-651.

[39] Shairi, N. A., B. H. Ahmad, and Peng Wen Wong. "Switchable radial stub resonator for isolation improvement of SPDT switch." *International Journal of Engineering and Technology (IJET)* 5, no. 1 (2013): 460-467.

[40] Chen, Haidong, Wenquan Che, Tianyu Zhang, Yue Chao, and Wengjie Feng. "SIW SPDT switch based on switchable HMSIW units." In *2016 IEEE International Workshop on Electromagnetics: Applications and Student Innovation Competition (iWEM)*, pp. 1-3. IEEE, 2016.